

## A new capsule technique for hydrothermal experiments using the piston-cylinder apparatus

JOHN C. AYERS,\* JAMES B. BRENNAN,\*\* E. BRUCE WATSON, DAVID A. WARK,  
WILLIAM G. MINARIK

Department of Earth and Environmental Sciences, Rensselaer Polytechnic Institute, Troy, New York 12180-3590, U.S.A.

### ABSTRACT

A new capsule technique has been developed to maintain a constant sample geometry at the high pressures and temperatures obtainable with a piston-cylinder apparatus. The capsule consists of a thick-walled transition metal cylinder, open on one end, and an inner noble metal sleeve. A noble metal lid welds to the capsule during cold pressurization, eliminating the need for arc welding to seal the loaded capsule. The high strength of the thick-walled capsules protects delicate samples such as single crystals during pressurization. At high temperature and pressure capsules shorten in the direction of compression but deform homogeneously. Pressure calibrations show that the pressure correction for the assembly is negligible. Ni powder can be used to buffer the  $f_{O_2}$  in an aqueous charge at NNO for >24 h at 1000 °C.

Applications of the capsule technique to hydrothermal experiments on single crystals are discussed. These experiments allow measurement of mineral solubilities, partition coefficients, and diffusion coefficients in minerals. Thick-walled capsules are also useful for experiments that require constant sample geometry, such as diffusion couples and textural studies.

### INTRODUCTION

There are very few data on the properties of COH fluids at pressures above 1.0 GPa. Because the piston cylinder can achieve pressures of 5.0 GPa (Boyd and England, 1960), it can be used to increase the range of conditions accessible for the study of fluids. However, the difficulties inherent in hydrothermal experiments on small samples have limited the use of the piston cylinder in studies of fluids. The usual procedure of sealing a fluid-bearing capsule shut by arc welding is unreliable because it may cause volatilization of an unknown mass of sample. Volatilization of caustic or radioactive fluids during welding is not only undesirable but also may change the bulk composition of the sample. Also, welded seals often fail during the experiment or the quenching process. The irregular shapes of capsules made in this fashion require that each has a custom-made receptacle, resulting in a different geometry in every experiment.

We have developed a capsule technique for mineral solubility measurements that avoids these problems. The capsule consists of an open-ended thick-walled transition-metal cylinder and a noble metal sleeve. During cold pressurization a noble metal lid seals the capsule shut, avoiding the step of welding the loaded capsule. The

strength of the thick-walled capsules protects fragile samples such as single crystals from being crushed during pressurization and maintains a constant sample geometry. Some applications of this capsule technique are discussed below.

### EXPERIMENTAL METHODS

#### Capsules

Capsules are made as follows. Form the inner sleeve by tri-crimping on one end a length of noble metal tubing (od 5.0 mm, id 4.6 mm, length 10 mm) and welding it shut (Fig. 1). Using a mandrel, tap the sleeve into a transition metal cylinder (od 6.3 mm, id 5.0 mm, outside length 9.0 mm, inside length 8.2 mm). Grind the open end of the capsule until the sleeve is flush with the cylinder, then clean the capsule and load the sample. Slide the open capsule into a crushable alumina container and cover with a noble metal lid (0.3–0.7 mm thick). Place an alumina disk on top to protect the thermocouple from contamination (Fig. 2). Then place the capsule and its receptacle in the piston cylinder assembly.

Capsule dimensions can be modified to suit experimental requirements, but the thickness of the noble metal lid is critical to the success of the experiment. For the quoted dimensions we found that a thickness of 0.5 mm is optimal. If it is thinner than 0.5 mm, the lid may shear above the inside lip and collapse into the capsule during pressurization, causing the capsule to leak. If it is thicker than 0.5 mm, it may support a significant differential

\* Present address: Geology Department, Vanderbilt University, Nashville, Tennessee 37235, U.S.A.

\*\* Present address: Geophysical Laboratory, Carnegie Institution of Washington, Washington, DC 20015-1305, U.S.A.

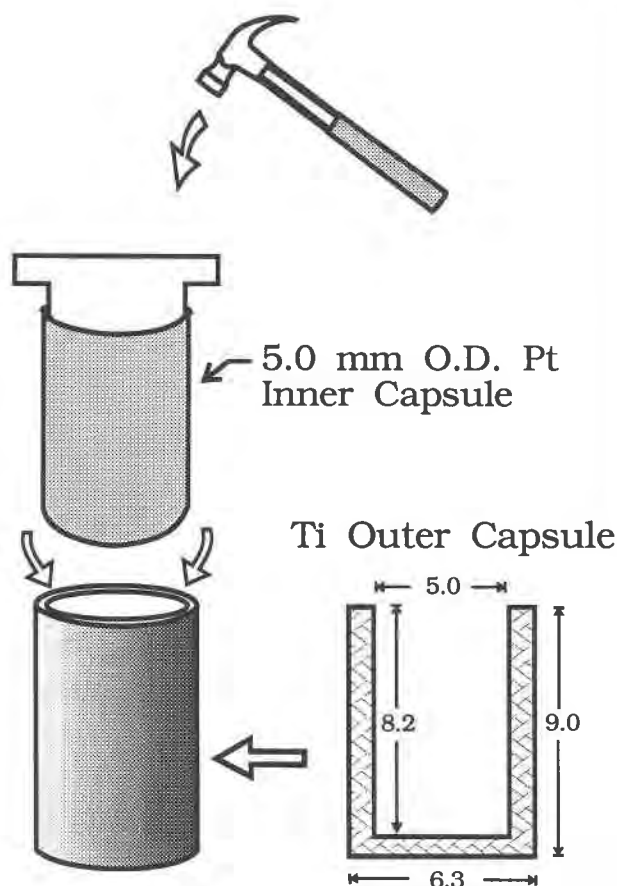


Fig. 1. Diagram showing the dimensions in millimeters of the transition metal (e.g., Ti) outer cylinder and how the noble metal (Pt) sleeve is tapped into it.

stress, which in fluid-bearing experiments may result in the capsule releasing fluid to eliminate any excess pressure from fluid. A lid of optimal thickness acts as a pressure membrane, expanding or collapsing until sample pressure is equal to the applied pressure.

Our experiments demonstrate that the lid forms a watertight seal with the open capsule during cold pressurization in the piston cylinder. When temperature is raised the lid alloys with the capsule, forming a permanent seal. This technique has been used by Ayers and Watson (1989, 1991) and Brenan and Watson (1989) to study mineral-fluid equilibria, and a variation was used by Watson (1991) to examine  $\text{CO}_2$  diffusion in hydrous melt. A different approach, taken by Cemič et al. (1990), is to hammer a tight-fitting lid into a thick-walled noble metal capsule. The technique described here is more cost effective but has a drawback. Diffusion of the transition metal into the sample container limits the useful life of the capsule. We discuss this problem below.

#### Sample pressure and temperature

To characterize experimental conditions, pressure and temperature calibrations of the capsule-bearing assembly

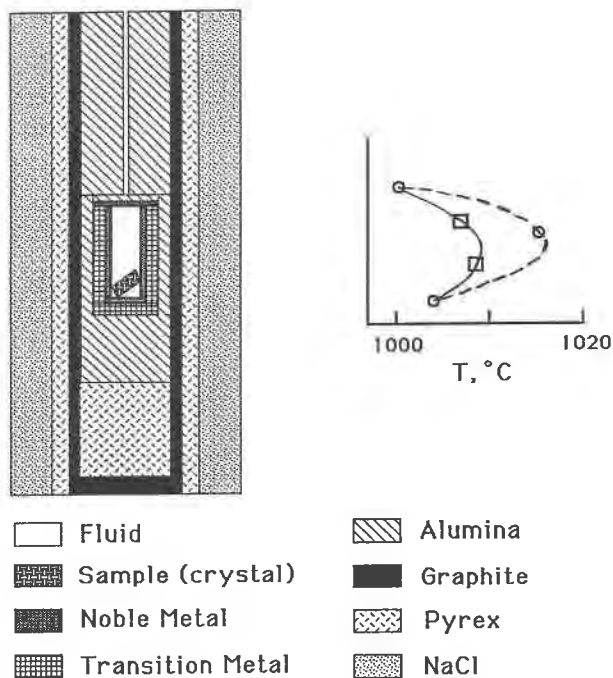


Fig. 2. Schematic cross section of the piston-cylinder assembly used for mineral solubility and  $f_{\text{O}_2}$  buffer measurements. Height of the assembly is 45 mm and diameter is 19.1 mm; all parts are proportionally sized. Materials are designated by markings explained in the key. The control thermocouple is positioned at the bottom of the hollow thermocouple well, directly above the capsule. Temperatures in the assembly are plotted at their corresponding vertical positions to illustrate the temperature gradient along the length of the sample (see text). Squares represent measurements made with the capsule in the assembly, and circles represent measurements without the capsule.

(Fig. 2) were performed. The temperature gradient along the long axis of the piston-cylinder assembly was determined from several experiments using two  $\text{WRe}_3\text{-WRe}_{25}$  (type D) thermocouples positioned at different distances from the top of the assembly. Sectioning of the assembly after the experiment allowed accurate measurement of the position of the two thermocouples. Measurements were made both with and without a thick-walled Ni capsule at 1.0 GPa, 1000 °C. When a thermocouple was placed inside an open capsule, it was surrounded by alumina to prevent contamination. Results show that the high thermal conductivity of the Ni capsule reduces the temperature gradient to 5 °C along the 8-mm sample length.

Pressure calibrations of the assembly using the falling sphere method allowed bracketing of the pressure of the NaCl melting curve at 1000 °C ( $\pm 10$  °C for the type D thermocouple used). Pure NaCl was loaded into a thick-walled Ti capsule with a Pt sphere near the top and a Pt lid above it. At 1000 °C, the nominal melting pressure is bracketed at  $0.905 \pm 0.025$  GPa for the piston-in technique and  $0.925 \pm 0.025$  GPa for the piston-out technique (Table 1). Interpolating the results of piston-in experiments by Cemič et al. (1990) and Bohlen (1984) at

TABLE 1. Results of pressure calibration

Technique*	T (°C)	P <sub>nom</sub> (GPa)	Results	1**	2**
P-in†	1000	0.93	solid	1009 °C	986 °C
P-in	1000	0.88	liquid		
P-out‡	1000	0.95	solid		
P-out	1000	0.90	liquid		

\* Pressure-calibration experiments used assembly shown in Figure 2 and the falling sphere technique. A Ti capsule contained NaCl, with a Pt sphere near the top and a Pt lid above it.

\*\* Results from other studies using the same technique: 1 = Cemič et al. (1990), who used a Ni-Cr thermocouple and cold-sealing noble metal capsules; 2 = Bohlen (1984), who used a Pt-Rh thermocouple and standard arc-welded Pt capsules. This study employed a W-Re thermocouple.

† Sample was cold-pressurized to 0.5 GPa, then pressure and temperature were raised simultaneously until the desired pressure and then the temperature were attained.

‡ Sample was cold-pressurized to 0.5 GPa, then pressure and temperature were raised simultaneously until pressure was 0.2 GPa over the desired pressure when the desired temperature was attained. Excess pressure was then slowly bled off.

0.905 GPa gives melting temperatures of 1009 and 986 °C, respectively, bracketing our results of 1000 ± 10 °C. The small differences in results are probably due to the different pressure corrections on emf for the thermocouples used (Ni-Cr by Cemič et al., 1990; Pt-Rh by Bohlen, 1984; W-Re, this study), errors in thermocouple calibrations (our calibration was supplied by the manufacturer), and the propagation of errors in the temperature and pressure readings.

By comparing results from internally heated experiments, Bohlen (1984) and Cemič et al. (1990) concluded that their assemblies had no pressure correction, i.e., they were frictionless. We therefore conclude that there is no pressure correction for our assemblies. The agreement between piston-in and piston-out results also suggests that the friction correction of the assembly is negligible (Bell and Williams, 1971).

### Experiments on fluids

Procedures are similar for all fluid-bearing experiments. The capsule (cylinder + sleeve) is loaded with known amounts of solid sample and fluid and placed in the assembly with its lid on top. Because the assembly is oriented as shown in Figure 2 when placed in the piston cylinder, gravity holds the lid on top of the capsule. The assembly is cold pressurized to 0.5 GPa to seal the capsule shut, then *P* and *T* are increased simultaneously until experimental conditions are reached (hot piston-in). A WRe<sub>3</sub>-WRe<sub>25</sub> thermocouple placed on top of the capsule controls temperature to ±5 °C, and pressure is manually maintained at ±5%. Turning the power off at the end of the experiment cools the sample rapidly to room temperature.

Recovered capsules are cleaned of any adhering alumina. The capsule is weighed, then the lid is punctured and fluid is retrieved for analysis. Drying the capsule at >100 °C and then reweighing it gives the final weight of H<sub>2</sub>O, which is always within 2% of the weight loaded, unless a buffer that consumes H<sub>2</sub>O in oxidation reactions

TABLE 2. Results of *f*<sub>O<sub>2</sub></sub> buffer measurements at 1.0 GPa, 1000 °C

id	SM	P	t (h)	t <sup>1/2</sup>	Δ <i>m</i> <sub>H<sub>2</sub>O</sub> (mg)
<i>f</i> <sub>O<sub>2</sub></sub> 8	Ni	Ni + NiO	3	1.73	5.00
<i>f</i> <sub>O<sub>2</sub></sub> 3	Ni	Ni + NiO	6	2.45	4.75
<i>f</i> <sub>O<sub>2</sub></sub> 4	Ni	Ni + NiO	12	3.46	10.59
<i>f</i> <sub>O<sub>2</sub></sub> 9	Ni	Ni + NiO	18	4.24	13.66
<i>f</i> <sub>O<sub>2</sub></sub> 1	Ni	Ni + NiO	24	4.90	15.46
<i>f</i> <sub>O<sub>2</sub></sub> 10	Fe <sub>3</sub> O <sub>4</sub> *	Fe <sub>3</sub> O <sub>4</sub> + Fe <sub>2</sub> O <sub>3</sub>	24	4.90	3.84

Note: SM is starting material, P is products (identified optically), and Δ*m*<sub>H<sub>2</sub>O</sub> is the mass loss of H<sub>2</sub>O. NNO experiments done in Ni capsules (od 6.3 mm, id 4.3 mm, outside length 10 mm, inside length 9.0 mm) with a Ni lid 1.0 mm thick. Roughly 60 mg of Ni powder also added to capsule. Log *f*<sub>O<sub>2</sub></sub> of NNO at 1.0 GPa and 1000 °C is -9.943 (Chou, 1987).

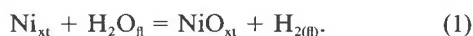
\* Fe<sub>3</sub>O<sub>4</sub> is magnetite (pure natural crystal powdered to approximately 10 μM), Fe<sub>2</sub>O<sub>3</sub> is hematite. Ni cylinder with Ag<sub>90</sub>Pd<sub>10</sub> sleeve and lid. Log *f*<sub>O<sub>2</sub></sub> of HM at 1.0 GPa and 1000 °C is -5.362 (Chou, 1987).

is present. The products of the experiment are retrieved by drilling a hole through the lid of the capsule or sawing off the lid.

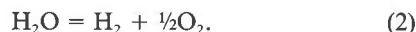
For H<sub>2</sub>O-CO<sub>2</sub> fluids, final weights of both H<sub>2</sub>O and CO<sub>2</sub> may be obtained as follows (Kerrick, 1974). After the experiment, weigh the capsule, freeze it in liquid N<sub>2</sub>, then puncture it and immediately measure its weight loss to get the mass of CO<sub>2</sub>. Dry the capsule and measure a second weight loss to get the mass of H<sub>2</sub>O.

### OXIDATION REACTIONS AND BUFFERING OF *f*<sub>O<sub>2</sub></sub>

Here we describe experiments designed to test the potential for buffering *f*<sub>O<sub>2</sub></sub> in fluid-bearing experiments. In experiments with sleeveless Ni capsules, we found that H<sub>2</sub>O oxidized exposed Ni to form NiO:



The value of *f*<sub>H<sub>2</sub></sub> is fixed by Reaction 1, which in turn fixes *f*<sub>O<sub>2</sub></sub> at the value of the Ni-NiO buffer through the reaction



Together, Reactions 1 and 2 buffer both *f*<sub>O<sub>2</sub></sub> and *f*<sub>H<sub>2</sub></sub> in the sample fluid. As Reaction 1 proceeds, H<sub>2</sub> diffuses out of the capsule because *f*<sub>H<sub>2</sub></sub> (assembly) < *f*<sub>H<sub>2</sub></sub> (sample). An experiment with magnetite + H<sub>2</sub>O yielded hematite, indicating *f*<sub>H<sub>2</sub></sub> (assembly) is even lower than the value set by the HM buffer when the activity of H<sub>2</sub>O is one (Table 2). The low ambient *f*<sub>H<sub>2</sub></sub> guarantees that H<sub>2</sub>O and CO<sub>2</sub> are the dominant species in a COH fluid.

To test whether oxidation reactions of this type could be used to buffer *f*<sub>O<sub>2</sub></sub> during experiments, we loaded Ni capsules (od 6.3 mm, id 4.3 mm, outside length 10 mm, inside length 9.0 mm) with finely powdered Ni metal and a weighed mass of H<sub>2</sub>O. A Ni lid 1.0 mm thick was placed on top. Experiments were conducted at 1.0 GPa and 1000 °C for different durations and, after each experiment, the mass of H<sub>2</sub>O remaining in the capsule was measured. The measured mass loss of H<sub>2</sub>O represents H<sub>2</sub> diffused out of the capsule and O<sub>2</sub> consumed by the buffer assemblage.

Measurements show that the mass loss of H<sub>2</sub>O, which

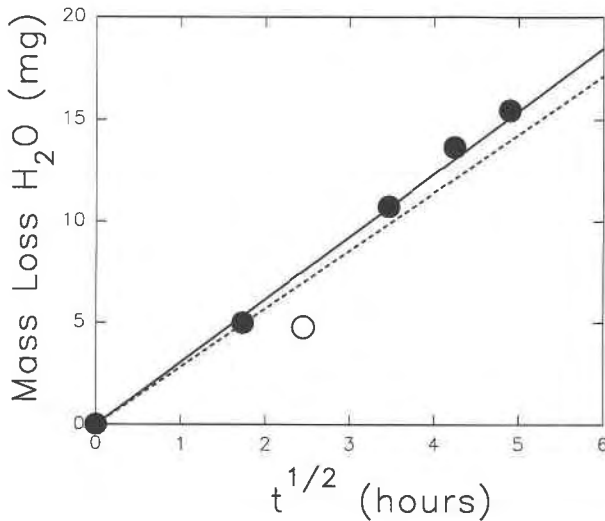


Fig. 3. Measured mass loss of H<sub>2</sub>O (mg) from oxidation of Ni plotted as a function of  $t^{1/2}$  (h) at 1.0 GPa and 1000 °C. Data from Table 2, including the boundary condition of zero mass loss at zero time. The hollow symbol appears to represent an outlier. Least squares regression yields slope  $m = 3.15$  when the hollow data point is not included (solid line), and  $m = 2.86$  when it is (dashed line). Capsule dimensions in text.

is a monitor of reaction progress, is linearly dependent on the square root of time (Fig. 3). That suggests that the rate-limiting step is diffusion of H<sub>2</sub> through the capsule walls. That must be the rate-limiting step (rather than reaction of the buffer assemblage) for  $f_{O_2}$  to be buffered to the equilibrium value for the buffer assemblage.

Because H<sub>2</sub> diffusion in metals is rapid at elevated temperatures (Chou, 1987), the rate of consumption of buffer and H<sub>2</sub>O is high. As shown in Table 2, oxidation of Ni consumes 15.5 mg of H<sub>2</sub>O in 24 h, over half the 30 mg of H<sub>2</sub>O normally loaded into these capsules. This rapid consumption of H<sub>2</sub>O limits the ability to buffer  $f_{O_2}$  in experiments longer than 24 h. The lifetime of  $f_{O_2}$ -buffered experiments may be extended by choosing buffers that in the presence of H<sub>2</sub>O set  $f_{H_2}$  closer to the ambient  $f_{H_2}$ , by increasing the ambient  $f_{H_2}$ , or by using capsule materials with lower H<sub>2</sub> diffusivities.

**CAPSULE MATERIALS**

Several elements may be used for the transition-metal cylinder and noble metal sleeve (Table 3). The noble metal sleeve temporarily isolates the sample from the reactive transition metal. At high temperature the transition metal diffuses through the noble metal sleeve and eventually reaches the sample, where it consumes H<sub>2</sub>O in oxidation reactions. Oxidation proceeds until no more H<sub>2</sub>O remains, and the capsule collapses. Capsule materials are therefore chosen to minimize the transition-metal flux and increase the potential lifetime of the capsule.

One way to increase capsule lifetimes is to choose metals that form intermediate alloys. Alloys form at the interface between the two metals and grow outward. When

**TABLE 3.** Utility of various metal combinations for thick-walled capsules

Cylinder	Sleeve	T (°C)	D* (cm <sup>2</sup> /s)	Lifetime (h)**	Max T (°C)
Ni	Pt	1100	1.2 E - 11	242	1455†
Ti	Pt	1000	5.7 E - 12	510	1310†
Ti	Pt	1200	9.4 E - 11	31	1310†
Nb	Pt	1000		>24	1700†
Ni	Ag <sub>80</sub> Pd <sub>20</sub>	1000	<1.1 E - 13	2.0E4	>962
Ti	Ag <sub>80</sub> Pd <sub>20</sub>				>962†
Ni	Au			>24‡	1000‡

\* Diffusivity of transition metal in noble metal. See text for method of calculation.

\*\* Minimum expected lifetime of capsule calculated from Equation 4 using the estimated diffusivity.

† Massalski (1990).

‡ Watson (1991).

these alloys are present, the net flux of transition metal through the noble metal is controlled not by the diffusivity alone but by the slower growth kinetics of the alloy layers. A good example is the binary system Ti-Pt, which forms at least two intermediate alloys (Fig. 4).

Minimum capsule lifetimes may be estimated from the diffusivity of the transition metal in the noble metal and the thickness of the noble metal (Table 3). Diffusivities were obtained from chemical diffusion profiles measured with a JEOL 733 electron microprobe. Operating conditions were 15-keV accelerating potential and 30-nA current, with a beam size of approximately 1 μm. Figures 4 and 5 show some measured chemical diffusion profiles. Solutions for planar geometries with infinite reservoirs were used to extract diffusivities from diffusion profiles. The planar approximation is valid because radial diffu-

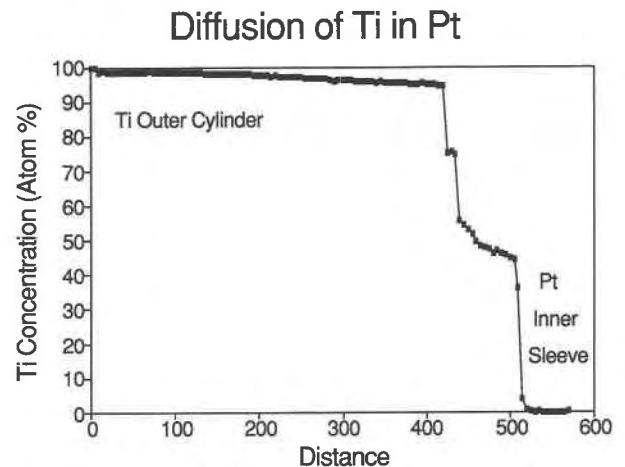


Fig. 4. Concentration profile of Ti across a Ti-Pt interface annealed at 1.0 GPa and 1200 °C for 20 h. Distance in micrometers. Ti from the outer cylinder and Pt from the inner sleeve interdiffuse and form several intermediate alloys, including Ti<sub>3</sub>Pt and TiPt. Formation of the alloy layers slows the diffusion of Ti into Pt and therefore extends the potential lifetime of the capsule. The net diffusivity of Ti is calculated to be 5.7 E - 12 cm<sup>2</sup>/s (see text).

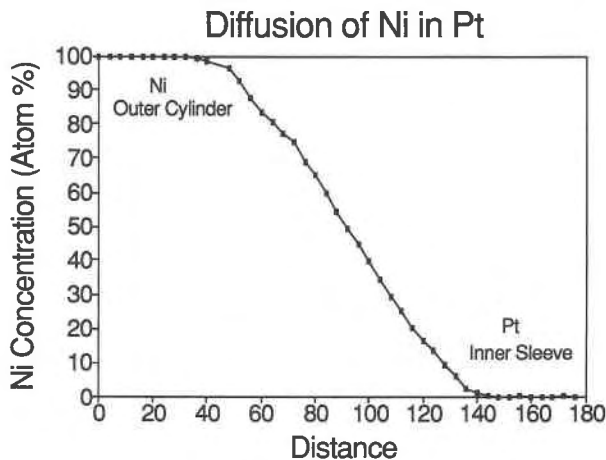


Fig. 5. Concentration profile across Ni-Pt interface annealed at 2.1 GPa and 1100 °C for 23 h. Distance in micrometers. Ni from the outer cylinder and Pt from the inner sleeve interdiffuse. The calculated diffusivity of Ni in Pt is  $1.2 \text{ E} - 11 \text{ cm}^2/\text{s}$  (see text).

sion distances are short compared to the radius of the capsule (Crank, 1975).

The diffusion of Ni into Pt is not complicated by the formation of intermediate compounds, but the profile is not a true error-function profile because it is convex, suggesting the diffusivity is concentration dependent (Fig. 5). A rough value of average  $D$  can be obtained from  $x^2 = 4Dt$ , where the diffusivity,  $D$ , is in  $\text{cm}^2/\text{s}$  and time,  $t$ , is the duration of the experiment in seconds. The variable  $x$  (cm) is the distance from the original interface at which the concentration of diffusing element is half the value at the interface (here 50 mol%). The original interface is the point where the net loss of diffusant on one side is equal to a net gain on the other.

For Ti diffusing into Pt, the diffusion length is small compared with the width of the zone of alloy formation (Fig. 4), suggesting that the growth of alloy layers slows the supply of Ti to the diffusion front. To obtain  $D$ , the distance  $x$  was set equal to the width of the alloy layers.

The minimum capsule lifetime was estimated from the diffusion equation for an infinite source with a fixed planar boundary, assuming constant surface concentration and diffusivity:

$$C(x,t) = \frac{C_1 - C_0}{2} \left[ 1 - \operatorname{erf}\left(\frac{x}{2\sqrt{Dt}}\right) \right] \quad (3)$$

where  $C_1$  and  $C_0$  are the initial atomic concentrations of Ti in the Ti metal and the Pt metal, respectively (Shewmon, 1963). Rearranging to solve for  $t$  in terms of the inverse error function and assigning a very low value to the concentration of the diffusing species [ $0.00001$ ,  $\operatorname{erf}(0.99999) = 3.9$ ] reduces the equation to

$$t_{\min} = \frac{1.05 \times 10^{-5}}{D} \quad (4)$$

Calculated capsule lifetimes are in reasonably good agreement with our practical experience with capsule failures. Also shown in Table 3 are the maximum recommended temperatures for each capsule type as evaluated from phase diagrams (Massalski, 1990). From these investigations we have concluded that Ti-Pt capsules are the most generally useful, with maximum temperatures of  $>1300 \text{ °C}$  and an expected lifetime of about 21 d at 1000 °C.

## APPLICATIONS

### Single crystal experiments

Previous piston-cylinder studies of the solubility of minerals in fluid (e.g., Schneider and Eggler, 1986) used the double-capsule (DC) technique of Anderson and Burnham (1965). This method is not sensitive enough to measure very low solubilities. In addition, it is difficult to tell if recrystallization in the temperature gradient of the piston-cylinder assembly has occurred (which results in overestimation of the solubility).

An alternate approach is to use a single crystal in direct contact with the fluid. The measured weight loss of the crystal combined with the mass of fluid yields the solubility. This technique is useful for measuring solubilities of minerals that dissolve congruently. However, single crystals contained in standard noble metal capsules are often crushed because these capsules deform extensively on pressurization. This fact, coupled with the problems of welding and containing fluids and of recognizing recrystallization, prompted the development of the thick-walled cold-sealing capsule for accurate measurements of mineral solubility (Ayers and Watson, 1989).

The trick to the single crystal technique is to place the crystal just below the hot spot of the assembly. This prevents dissolution and reprecipitation of the crystal to the cold end of the capsule (Fig. 2). Because the thermocouple is roughly the same distance above the furnace hot spot as the crystal is below, it measures the approximate temperature of the crystal.

The single crystal technique has been used to measure the solubilities of accessory minerals (Ayers and Watson 1989, 1991) and some rock-forming silicates (Brenan and Watson, 1989) in supercritical aqueous fluids. A similar technique was used by Becker et al. (1983) to measure the solubility of corundum in  $\text{H}_2\text{O}$ . These studies show that, within error,  $<24 \text{ h}$  are needed to reach solubility equilibrium at 1000 °C using single crystals. For the single crystal and DC techniques, equilibrium is tested by measuring solubility as a function of time. Neither method allows testing for equilibrium by reversing the approach to equilibrium (Barnes, 1981), which would involve growing crystals from a supersaturated solution.

Repeated attempts at using an inner capsule within the thick-walled cold-sealing capsules failed. The inner capsule always welds to or is pinched by the sleeve so that it cannot be retrieved. However, measurements of rutile solubility using standard thin-walled Pt double capsules

show good agreement with single crystal determinations in both thick-walled Ti-Pt and thin-walled Pt capsules (Ayers, 1991).

The single crystal technique has been found to be more sensitive (solubilities as low as 0.05 wt% for a balance, with a precision of  $\pm 0.01$  mg) than the DC technique. Also, multiple determinations show good precision for minerals that dissolve congruently. However, there are several potential sources of error in single-crystal solubility measurements, as discussed in Becker et al. (1983). Some care is required, but it is usually possible to minimize or eliminate these errors by carefully examining the sample and by taking certain precautions.

Once equilibrium is achieved, the only way that mineral solubilities can be underestimated is if material grows epitaxially on the surface of the crystal during the quenching process. That is considered unlikely, since during the quenching process crystals grow at a high degree of undercooling, which typically results in rapid nucleation and therefore formation of many small crystals (Zhang and Nancollas, 1991). Single crystal experiments on various minerals (Ayers, 1991; Ayers and Watson, 1991) have produced several lines of evidence to indicate that the stable crystal does not grow significantly during the quenching process. Electron microprobe analyses show that quench solutes have variable compositions and are frequently chemically zoned. Solute usually consists of very small crystals that frequently contain fluid inclusions. In contrast, the crystal shows no evidence of chemical zoning or fluid inclusions near its surface. The good agreement between solubilities measured using single crystal and DC techniques suggests that quench overgrowth does not significantly affect the results of single crystal experiments (Ayers, 1991). Only very limited quench overgrowth can occur in DC experiments because residual crystals are isolated from the bulk of the fluid during the quenching process.

Solubilities may be overestimated if recrystallization, breakage, or chipping of crystals occurs. Recrystallization in the temperature gradient of the capsule can be recognized by an accumulation of large, euhedral crystals at the cold end of the capsule and by extreme dissolution features on the surface of the large single crystal where it is closest to the hot spot. Because single crystals initially have euhedral natural faces or are cut into perfect cubes, careful examination of the crystal surface after the experiment reveals whether chipping or breakage has occurred. Because of these problems, solubilities measured using the single crystal technique are considered maximum estimates.

For insoluble minerals, single crystals may be used to measure simultaneously aqueous mineral solubilities, partition coefficients, and crystalline diffusion coefficients. This is accomplished by partially equilibrating a crystal with a doped fluid, measuring the weight loss of the crystal for the solubility, and then measuring the diffusion profile in the crystal using a high-sensitivity, *in situ*, microanalytical technique. The diffusion profile yields

the diffusivity and surface concentration, and the latter combined with the concentration in the fluid gives the partition coefficient. This method has been used with Rutherford backscattering to measure apatite solubility, along with the apatite-fluid partition coefficient and diffusivity of U in apatite (Ayers et al., unpublished data).

There are several ways to investigate systems more complex than fluid + one mineral. Fluids may be pre-saturated with a phase by grinding the phase into a very fine powder, to promote rapid dissolution. Also, more than one crystal can be loaded so that mineral solubilities may be obtained simultaneously. That allows study of fluid-rock equilibria by measuring the amount of each phase that dissolves in the fluid. Adding up the contributions of each mineral allows an estimate of the fluid composition. There are a few potential problems with this technique. Silicates tend to dissolve incongruently and are prone to recrystallization in the temperature gradient of the piston cylinder (Brenan, 1990). Several minerals may contain common chemical components, and by propagation of errors this may lead to a large error in the estimated fluid composition. However, for experiments on silicate assemblages, there should be enough quench solute to analyze, providing a better estimate of fluid composition.

#### Chemical interdiffusion measurements

A general requirement of diffusion experiments is that the sample have a simple, fixed geometry. That allows for an analytical solution of the diffusivity based on concentration-distance relations relative to the source of a diffusing species with a specified geometric shape. As discussed above, we have examined chemical interdiffusion of the metals composing the capsule. Here we discuss two other types of diffusion experiments that use the cold-sealing capsule technique.

In his study of tracer diffusion of CO<sub>2</sub> and Cl in hydrous silicate melts, Watson (1991) used thick-walled capsules in a two-step process. A hydrous glass was synthesized by loading a thick-walled capsule lined with noble metal with silicate powder + H<sub>2</sub>O, covering the capsule with a lid and subjecting the sample to high *P* and *T* in the piston cylinder. After retrieving the capsule and cutting off the lid, the surface of the capsule was polished. Radiotracer-bearing solutions of the diffusing species were applied to the polished surface of the glass, and a lid was placed on top. Again the capsule was subjected to high *P* and *T* for a specified duration and then retrieved. The capsule was sectioned lengthwise, polished, and then exposed to nuclear emulsion plates to record the diffusion profiles as  $\beta$ -track maps (Watson, 1991).

A variation on this technique is used to measure chemical interdiffusion between silicate melts or fluid-bearing rocks of different compositions. By drilling two holes in the capsule, two samples of different compositions may be loaded in the capsule and pretreated at *P* and *T* (to synthesize a homogenous glass, etc.). After the synthesis step, the capsule is cut perpendicular to the long axis of



the cylinders, and each half is polished. Rotating one half 180° relative to the other juxtaposes the two samples when the halves are rejoined. The capsule is again subjected to *P* and *T* to form the diffusion couple, then is retrieved and sectioned lengthwise (perpendicular to the interface), polished, and characterized.

### Other potential uses

The constant sample geometry afforded by cold-sealed capsules opens the possibility of conductance cell measurements on fluids in the piston cylinder. The lid serves as one electrode and the capsule as the other. The two electrodes are separated by an electrical insulator such as alumina, which acts as a gasket between the electrodes and is in contact with the sample. The entire conductance cell is surrounded by alumina to prevent current leakage. In preliminary experiments we found it very difficult to seal fluids in capsules with alumina or ceramic gaskets, but we did succeed in making a few measurements of the electrical resistivity of salt at pressure and temperature.

Thick-walled capsules may be used to apply a hydrostatic pressure, by means of an intervening fluid, on a sample at conditions where normal solid media retain strength. This is accomplished by loading a sealed capsule containing the sample into a larger cold-sealing capsule containing fluid. The outer capsule also may be loaded with the appropriate buffers. The fluid acts as a hydrostatic pressure medium (Cemič et al., 1990).

Another application of the capsules is in textural studies. Because the capsules maintain their shape even during the quenching process, they preserve the textural relations present at experimental conditions. After the experiment the capsule may be sawed open lengthwise, and the sampled impregnated with epoxy before polishing. Experiments of this type have been done on accessory mineral-peridotite-H<sub>2</sub>O systems to characterize phase equilibria and textural relations (Ayers, 1991, and unpublished data). A similar technique was employed by Wark and Stimac (1992) in their study of dissolution of oriented single crystals of alkali feldspar in silicate melt and the resulting formation of rapakivi texture.

### ACKNOWLEDGMENTS

This paper represents part of the first author's Ph.D. thesis at Rensselaer Polytechnic Institute. We thank John Holloway and L. Cemič for their helpful reviews. Funding for this study was provided by NSF grant no. EAR-8904177 to E.B.W. and a Mineralogical Society of America Biennial Research grant to J.C.A.

### REFERENCES CITED

Anderson, G.M., and Burnham, C.W. (1965) The solubility of quartz in supercritical water. *American Journal of Science*, 263, 494–511.  
 Ayers, J.C. (1991) Experimental studies of the chemistry of aqueous fluid-accessory mineral systems at high *P-T* conditions with implications for

fluid-rock interactions, 212 p. Ph.D. thesis, Rensselaer Polytechnic Institute, Troy, New York.  
 Ayers, J.C., and Watson, E.B. (1989) Solubility of accessory minerals in H<sub>2</sub>O at upper mantle conditions. *Eos*, 70, 506.  
 ——— (1991) Solubility of apatite, monazite, zircon, and rutile in supercritical aqueous fluids with implications for subduction zone geochemistry. *Philosophical Transactions of the Royal Society of London A*, 335, 365–375.  
 Barnes, H.L. (1981) Measuring thermodynamically-interpretable solubilities at high pressures and temperatures. In D. Rickard and F. Wickman, Eds., *Chemistry and geochemistry of solutions at high temperatures and pressures, physics and chemistry of the Earth*, vol. 13–14, p. 321–343. Pergamon Press, New York.  
 Becker, K.H., Cemič, L., and Langer, K.E.O.E. (1983) Solubility of corundum in supercritical water. *Geochimica et Cosmochimica Acta*, 47, 1573–1578.  
 Bell, P.M., and Williams, D.W. (1971) Pressure calibration in piston-cylinder apparatus at high temperature. In G.C. Ulmer, Ed., *Research techniques for high pressure and high temperature*, p. 195–216. Springer-Verlag, New York.  
 Bohlen, S.R. (1984) Equilibria for precise pressure calibration and a frictionless furnace assembly for the piston-cylinder apparatus. *Neues Jahrbuch für Mineralogie Monatshefte*, 9, 404–412.  
 Boyd, F.R., and England, J.L. (1960) Apparatus for phase-equilibrium measurements at pressures up to 50 Kb and temperatures up to 1750 °C. *Journal of Geophysical Research*, 65, 741–748.  
 Brenan, J.B. (1990) Partitioning of trace elements between mantle minerals and non-silicate fluids at high *P-T* conditions, 242 p. Ph.D. thesis, Rensselaer Polytechnic Institute, Troy, New York.  
 Brenan, J.B., and Watson, E.B. (1989) High *P-T* solubility of olivine, orthopyroxene, and Cr-diopside in H<sub>2</sub>O and H<sub>2</sub>O-CO<sub>2</sub> fluids: Experimental techniques and preliminary results. *GAC-MAC Program with Abstracts*, 14, A94.  
 Cemič, L., Geiger, C.A., Hoyer, W.W., Koch-Müller, M., and Langer, K. (1990) Piston-cylinder techniques: Pressure and temperature calibration of a pyrophyllite-based assembly by means of DTA measurements, a salt-based assembly, and a cold sealing sample encapsulation method. *Neues Jahrbuch für Mineralogie Monatshefte*, 2, 49–64.  
 Chou, I.M. (1987) Oxygen buffer and hydrogen sensor techniques at elevated pressures and temperatures. In G.C. Ulmer and H.L. Barnes, Eds., *Hydrothermal experimental techniques*, p. 61–99. Wiley, New York.  
 Crank, J. (1975) *The mathematics of diffusion*, 414 p. Clarendon Press, Oxford.  
 Kerrick, D.M. (1974) Review of metamorphic mixed-volatile (H<sub>2</sub>O-CO<sub>2</sub>) equilibria. *American Mineralogist*, 59, 729–762.  
 Massalski, T.B., Ed. (1990) *Binary alloy phase diagrams* (2nd edition). ASM International, Metals Park, Ohio.  
 Schneider, M.E., and Eggler, D.H. (1986) Fluids in equilibrium with peridotite: Implications for mantle metasomatism. *Geochimica et Cosmochimica Acta*, 50, 711–724.  
 Shewmon, P.G. (1963) *Diffusion in solids*, 203 p. McGraw-Hill, New York.  
 Wark, D.A., and Stimac, J.A. (1992) Origin of mantled (rapakivi) feldspars: Experimental evidence of a dissolution- and diffusion-controlled mechanism. *Contributions to Mineralogy and Petrology*, in press.  
 Watson, E.B. (1991) Diffusion of dissolved CO<sub>2</sub> and Cl in hydrous silicic to intermediate magmas. *Geochimica et Cosmochimica Acta*, 55, 1897–1902.  
 Zhang, J.W., and Nancollas, G.H. (1991) Mechanisms of growth and dissolution of sparingly soluble salts. In *Mineralogical Society of America Reviews in Mineralogy*, 23, 365–396.

MANUSCRIPT RECEIVED OCTOBER 25, 1991

MANUSCRIPT ACCEPTED APRIL 28, 1992